

False vacuum decay in quantum spin chains

Gianluca Lagnese,^{1,2} Federica Maria Surace,^{1,3} Márton Kormos,^{4,5} and Pasquale Calabrese^{1,2,3}

¹SISSA, via Bonomea 265, 34136 Trieste, Italy

²INFN, Sezione di Trieste, 34136 Trieste, Italy

³International Centre for Theoretical Physics (ICTP), Strada Costiera 11, 34151 Trieste, Italy

⁴MTA-BME Quantum-Dynamics and Correlations Research Group, Eötvös Loránd Research Network (ELKH), Budapest University of Technology and Economics, 1111 Budapest, Budafoki út 8, Hungary

⁵BME “Momentum” Statistical Field Theory Research Group, Institute of Physics, Budapest University of Technology and Economics, 1111 Budapest, Budafoki út 8, Hungary

(Dated: January 5, 2022)

The false vacuum decay has been a central theme in physics for half a century with applications to cosmology and to the theory of fundamental interactions. This fascinating phenomenon is even more intriguing when combined with the confinement of elementary particles. Due to the astronomical time scales involved, the research has so far focused on theoretical aspects of this decay. The purpose of this Letter is to show that the false vacuum decay is accessible to current optical experiments as quantum analog simulators of spin chains with confinement of the elementary excitations, which mimic the high energy phenomenology but in one spatial dimension. We study the non-equilibrium dynamics of the false vacuum in a quantum Ising chain and in an XXZ ladder. The false vacuum is the metastable state that arises in the ferromagnetic phase of the model when the symmetry is explicitly broken by a longitudinal field. This state decays through the formation of “bubbles” of true vacuum. Using iTEBD simulations, we are able to study the real-time evolution in the thermodynamic limit and measure the decay rate of local observables. We find that the numerical results agree with the theoretical prediction that the decay rate is exponentially small in the inverse of the longitudinal field.

The possibility that our universe, as it cooled down, may have settled into a metastable state (false vacuum) that may eventually decay was proposed by Coleman in 1977 and has been since then one of the most popularized ideas of physical cosmology [1–4]. The decay would happen through bubble nucleation, i.e. the formation of bubbles of true vacuum that rapidly expand: the probability for this process to occur is extremely small, and studying this phenomenon is notoriously challenging due to its intrinsic non-perturbative character.

Recently, the possibility of using tools from quantum technologies for studying problems of strongly coupled quantum field theories has attracted a lot of interest [5–8]. On the one hand, tensor-network approaches are promising candidates for studying non-equilibrium properties that cannot be accessed with traditional Monte Carlo simulations. These approaches have been successfully applied to 1+1 and 2+1 dimensional lattice gauge theories [9–16] but they suffer from limitations with dimensionality. Therefore, there has been an increasing interest in the toolbox of quantum simulators [17–23]. The hope is that controllable quantum systems in table-top experiments will help us understand difficult problems in quantum field theory, including, for example, the decay of the false vacuum [24–28].

In this context, one-dimensional quantum spin models represent the ideal framework for benchmarking quantum simulators: they can host particle confinement [29, 30], a property that can be observed in the non-equilibrium dynamics after a quantum quench [31–33]; it has also been suggested that their real-time evolution can reveal in-

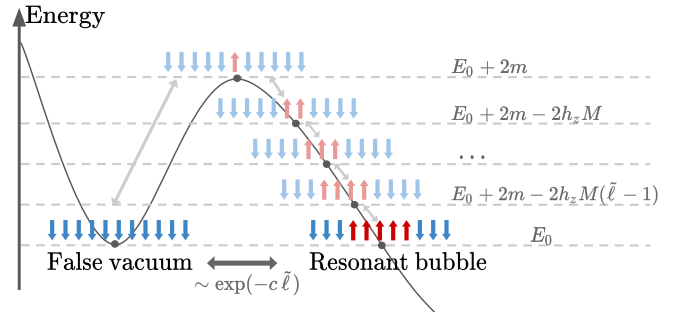


FIG. 1: Illustration of bubble formation (false vacuum is in blue, true vacuum in red). The process that leads to the resonant bubble goes through $O(\tilde{\ell})$ off-resonant states: a small bubble is (virtually) created and expanded until it reaches the resonant size $\tilde{\ell}$. As a consequence, the matrix element that drives the false vacuum decay is exponentially small in $\tilde{\ell} \propto h_z^{-1}$.

teresting phenomena including collisions of particles and bubble nucleation [34–39].

Here, we propose to study the decay of the false vacuum in quantum spin models using simulations of real-time dynamics after a quantum quench.

False vacuum decay— To illustrate the phenomenon of false vacuum decay we consider a prototypical model for confinement, the quantum Ising chain in transverse and longitudinal field, with Hamiltonian

$$H(h_x, h_z) = - \sum_i (\sigma_i^z \sigma_{i+1}^z + h_x \sigma_i^x + h_z \sigma_i^z), \quad (1)$$

where σ_i^α are Pauli operators, and the amplitudes h_x and h_z are the transverse and longitudinal field, respectively.

For $h_z = 0$ the model has a \mathbb{Z}_2 symmetry that is spontaneously broken for $|h_x| < 1$ (ferromagnetic phase). In this phase there are two ground states characterized by opposite magnetizations $\langle \sigma_i^z \rangle = \pm M$, with $M = (1 - h_x^2)^{1/8}$ [40]. The model is diagonalized with a mapping to free fermions: the corresponding excitations in the ferromagnetic phase are kinks that interpolate between domains with opposite magnetization [41]. The kinks can propagate freely and have dispersion relation

$$\omega(\theta) = 2(1 - 2h_x \cos \theta + h_x^2)^{1/2}. \quad (2)$$

For a longitudinal field $h_z \neq 0$, the \mathbb{Z}_2 symmetry is explicitly broken and the degeneracy between the two ground states is split by an extensive quantity $\sim 2h_z MN$, where N is the number of sites in the chain: the state with magnetization aligned with the external field (the *true vacuum*) is the ground state of the model, while the one with opposite magnetization (the *false vacuum*) is a metastable state. The nature of the excitations is also drastically modified: the longitudinal field induces a linear potential between the kinks, confining them into *mesons* [29]. The confinement strongly affects many aspects of the non-equilibrium dynamics [31–36, 42–52].

The false vacuum is at high energy, so it can resonantly decay into the continuum of multi-meson states. While this decay is a very complicated process, the basic mechanism can be understood as the formation of bubbles of true vacuum in the system. Creating a bubble of size ℓ requires the energy given by the masses of the two kinks lowered by $2h_z M \ell$. When this energy becomes zero, the bubble is resonantly excited. This bubble can then further decay through other resonant processes. However, for h_z sufficiently small, the phenomenon of bubble formation is very slow. This slowness can be understood by the following simple heuristic argument. A resonant bubble of size ℓ results from the frequent creation of a small bubble (of size of order 1) that then should expand until it reaches the resonant size $\tilde{\ell} \gg 1$ (see Fig. 1). This expansion is a high-order process in the perturbation theory in h_z and, as a consequence, the matrix element for exciting the resonant bubble is exponentially small in $\tilde{\ell} \propto h_z^{-1}$.

The decay of the metastable false vacuum in the Ising chain has been studied in Ref. 53, where the following expression of the decay rate per site was obtained [72]:

$$\gamma = \frac{\pi}{9} h_z M \exp\left(-\frac{q}{h_z}\right) \quad (3)$$

with $q = |f(-i \ln h_x)|/M$ and $f(\theta) = 2 \int_0^\theta \omega(\alpha) d\alpha$. Note that q and M only depend on h_x . This rate γ can be interpreted as the number of resonant bubbles that are created per unit time divided by the number of sites. In agreement with the argument explained above, the

decay is non-perturbative in the longitudinal field, with an exponential dependence on h_z^{-1} .

We note that an analogous mechanism drives the phenomenon known as *string breaking*. String breaking is typically understood as the saturation of the effective interaction between two static charges (or kinks, in this case) at large distance, due to the screening effects of other charges: in other words, the string that extends between the two static charges is broken by the creation of dynamical charges. In the model we are studying, the string corresponds to a false vacuum domain and the string breaking effect corresponds to the formation of a bubble in the domain. The dynamics of string breaking has been studied in this model, in other spin chains, and lattice gauge theories [21, 54–68], and similar expressions for the decay rate were found.

Quench protocol and methods— The goal of this Letter is to show that a window of Hamiltonian parameters of the Ising spin chain (h_x, h_z) exists such that the false vacuum decay can be observed through numerical simulations of the non-equilibrium dynamics after a quantum quench. The quench protocol is the following: i) we prepare the system in the ferromagnetic state with all the spins in the $\sigma_i^z = 1$ direction; ii) we evolve the system in imaginary time with the Hamiltonian $H(h_x, -h_z)$ using infinite volume time evolving block decimation (iTEBD) until we achieve a good convergence to the ground state; iii) we quench $-h_z \rightarrow h_z$ and evolve in real time. Using this protocol, we are able to prepare the false vacuum of $H(h_x, h_z)$ and study its evolution in real time using iTEBD. The state preparation ii) is obtained using a Trotter step $\delta t = 10^{-3}$, and the imaginary time evolution stops when the relative change of the energy density is smaller than 10^{-16} . The real time evolution after the quench iii) is performed with a Trotter step $\delta t = 10^{-2}$. The bond dimension χ is set to 512. We checked the stability of the numerical simulations with respect to changes in χ and δt .

We stress that in our quench protocol the false vacuum decay drives the system toward a thermal state, that has a finite energy density with respect to the true vacuum. Only in the limit $h_z \rightarrow 0$ this state tends to the true vacuum.

Time scales— Before embarking on the analysis of the numerical data, we should have a clear picture of all the time scales entering in the quench dynamics of our model. Starting from the false vacuum, the first process happening is the creation of off-resonant bubbles. During this (relatively) short-time transient, say up to time τ_r , the system remains effectively frozen in the false vacuum until the resonant bubbles start being produced. However, here we are not interested in this transient but only in the growth of the resonant bubbles, because this is the process that leads to the false vacuum decay described by the rate (3). For the accurate measurement of this rate, we need a clear separation of this time scale

from the successive ones. Indeed, at very late time, when most of the false vacuum decayed, since the system is at finite energy density, it starts thermalizing through the propagating states that originate from the decay of the resonant bubbles: the late time dynamics is governed by the thermal state corresponding to the energy of the pre-quench state (only for very small h_z this is close to zero temperature, i.e. the true vacuum). We denote with τ_D the time scale for the onset of thermalization; unfortunately, we do not know how to estimate τ_D , but its determination lies beyond the scope of this Letter.

We emphasize that Eq. (3) is expected to work well under the assumption of a clean separation of time scales, i.e. $\tau_r \ll \gamma^{-1} \ll \tau_D$. For the Hamiltonian (1), such separation of time scales is guaranteed in the regime $h_z \ll 1$ and h_x not too close to 1. The requirement $h_z \ll 1$ is obvious, since as h_z grows all the above time scales $\tau_r, \gamma^{-1}, \tau_D$ become of order one and there cannot be any separation. Moreover, if h_x gets too close to 1, the masses of the kinks become very small and the assumption that the false vacuum preferably decays into one-domain states (resonant bubbles) is no longer justified.

In conclusion, the false vacuum decay is expected to be described by Eq. (3) in the limit of small h_z and h_x not too close to 1. However, as the fields are reduced, the time scale γ^{-1} soon becomes extremely large (which is the reason why false vacuum decay is generically an elusive phenomenon, see also [69]). Thus the main difficulty of the numerical analysis is to find a window of the Hamiltonian parameters such that there is an optimal balance between a reasonable separation of time scales (to have a time range in which Eq. (3) describes something) and its numerical accessibility. We found that such balance is obtained for rather small h_z (of the order of 10^{-2}), but with h_x relatively large $h_x \sim [0.7, 0.9]$: a smaller h_x makes the decay time (γ^{-1}) too long and a larger h_z destroys completely the time-scale separation.

Results— To estimate the decay rate, we analyze the following two observables

$$F(t) = \frac{\langle \sigma_i^z(t) \rangle + \langle \sigma_i^z(0) \rangle}{2\langle \sigma_i^z(0) \rangle}, \quad (4)$$

$$G(t) = 1 - \|\rho(t) - \rho(0)\|_1, \quad (5)$$

where $\rho(t)$ is the two-site density matrix at time t and $\|\rho(t) - \rho(0)\|_1$ is the trace distance between the two density matrices. Both quantities can be easily computed in iTEBD, and satisfy $F(0) = G(0) = 1$, while they vanish in the true vacuum. The time evolution of $F(t)$ is fully encoded in the magnetization and, consequently, is expected to decay with a rate

$$\gamma_F \simeq \gamma_{\tilde{\ell}} = \frac{f(\pi)}{18} \exp\left(-\frac{q}{h_z}\right), \quad (6)$$

where the size of the resonant bubble is $\tilde{\ell} = \frac{f(\pi)}{2h_z M \pi}$ (see Ref. 53). Note that for small h_z , this rate is much larger

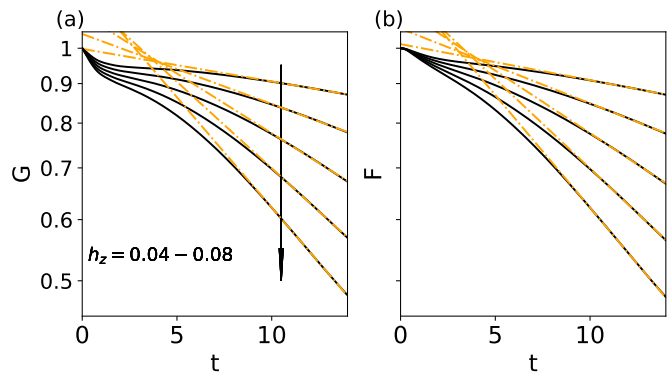


FIG. 2: *False vacuum decay in the quantum Ising chain.* The time evolution of $F(t)$ and $G(t)$, in Eqs. (4) and (5), is shown for $h_x = 0.8$ and different values of h_z after the quench $-h_z \rightarrow h_z$. The dot-dashed lines are the exponential fits in the decay region performed to extract the decay rates γ_F and γ_G .

than γ , so the time scale needed to observe the decay in our simulation is significantly reduced.

As an illustrative example for the determination of the decay rates of F and G , in Fig. 2 we report their evolution at fixed $h_x = 0.8$ and different values of h_z on a semi-log scale. It is evident that after a short transient, all the data show a distinct exponential decay (linear behavior on semi-log scale).

For all the considered values of h_x and h_z , we performed an exponential fit $O(t) = A_O e^{-\gamma_O t}$, with $O = F, G$. The fit is done in a time range $t_0 < t < t_1$ and then we check the stability of the fit for small variations of t_0, t_1 . The resulting decay rates $\gamma_{F,G}$ are plotted in Fig. 3-a,b,c as functions of h_z^{-1} again on semi-log scale. The exponential dependence on $1/h_z$, expected from Eq. (6), is very clear in the data. We fitted these rates with

$$\gamma_O = k_O e^{-q_O/h_z}, \quad O = F, G. \quad (7)$$

In Fig. 3-d we report the obtained coefficients q_F, q_G : they are compatible with each other and they both agree very well with the theoretical prediction $q = |f(-i \ln h_x)|/M$ in the full range of h_x considered. The prefactors k_F and k_G in Eq. (7) turn out to be different from what predicted by Eq. (6) (the data in Fig. 3-a,b,c are shifted compared to the dashed line). However, this shift is not surprising at all because we know that (i) the prefactor depends on the specific observable (e.g., compare Eqs. (3) and (6)), (ii) we expect it to be more affected by the approximations done in the derivation of Eq. (6).

XXZ ladder— To show the general validity of our analysis, we consider a second model presenting confine-

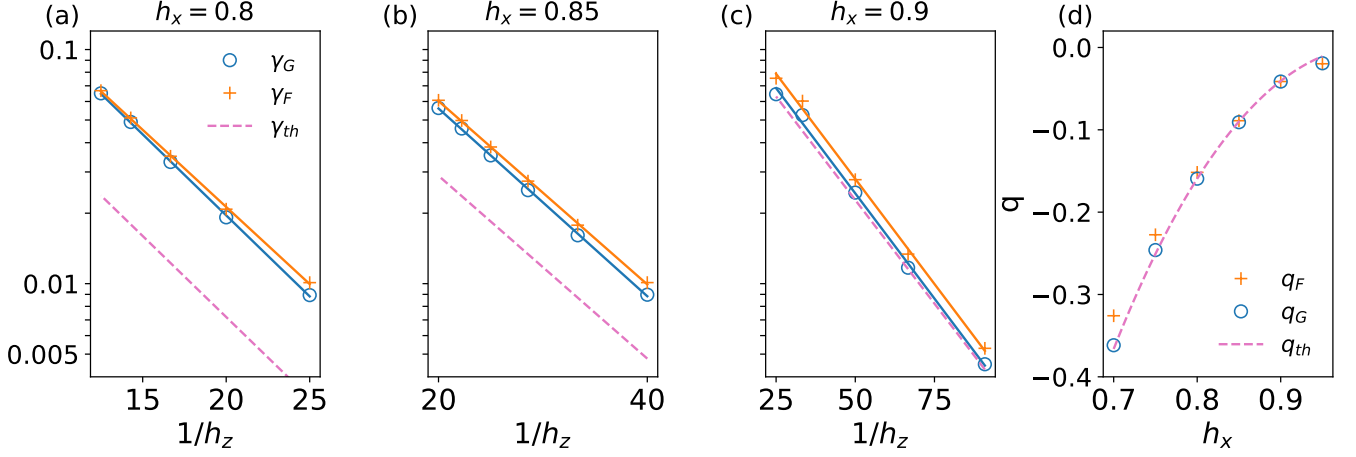


FIG. 3: *Decay rates in the quantum Ising chain.* In panels (a),(b),(c) we show the decay rates γ_F, γ_G , obtained from the fits of $F(t), G(t)$ as in Fig. 2. The continuous lines are the fits of the exponential dependence of the rates in $1/h_z$. The dashed line represents the theoretical prediction (6). From the fits the coefficients q_F and q_G are extrapolated and showed against the theoretical value $q_{th} = |f(-i \ln h_x)|/M$ (dashed line) in panel (d).

ment of elementary excitations with hamiltonian [70]

$$H(\Delta_{||}, \Delta_{\perp}) = \frac{1}{2} \sum_{j=1}^L \sum_{\alpha=1,2} [\sigma_{j,\alpha}^x \sigma_{j+1,\alpha}^x + \sigma_{j,\alpha}^y \sigma_{j+1,\alpha}^y + \Delta_{||} \sigma_{j,\alpha}^z \sigma_{j+1,\alpha}^z] + \Delta_{\perp} \sum_{j=1}^L \sigma_{j,2}^z \sigma_{j,1}^z \quad (8)$$

i.e. two XXZ spin-1/2 chains coupled along the longitudinal direction through an anisotropic Ising-like interaction. Compared to the Ising spin chain (1), the model possesses two interesting features. The first is that in the absence of the confining interaction (h_z and Δ_{\perp}), the Ising spin chain becomes a free model, while the decoupled XXZ chains constitute an interacting (integrable) spin model. The second one is that confinement is induced by the internal interaction between the chains, a built-in mechanism, instead of an external field (and this is more similar to what happens for quarks). We work in the gapped anti-ferromagnetic phase, i.e. $\Delta_{||} \in (1, +\infty)$ where the model for $\Delta_{\perp} = 0$ has four degenerate anti-ferromagnetic ground states. The confining potential explicitly breaks the original $\mathbb{Z}_2 \times \mathbb{Z}_2$ symmetry to a single \mathbb{Z}_2 [70]: the four degenerate ground states at $\Delta_{\perp} = 0$ are split in two doublets separated by an energy of the order $\Delta_{\perp} L$. The two lowest states (the true vacua) are now the stable ground states, while the other two (the false vacua) are metastable states at high energy and can decay in the continuum of the many-body spectrum.

In analogy with the Ising model, we prepare the false vacuum as the ground state at $-\Delta_{\perp}$ and then we quench $-\Delta_{\perp} \rightarrow \Delta_{\perp}$. For several values of the interactions Δ_{\perp} and $\Delta_{||}$, we extract the decay rates $\gamma_{F,G}$ for $F(t), G(t)$ (here F in Eq. (4) is built with the staggered magnetization and G in Eq. (5) with the reduced density matrix

of two adjacent rungs). In Fig. 4, a) and b), we show the time evolution of G after the quench for two values of $\Delta_{||}$. Even though we do not have analytic predictions for this

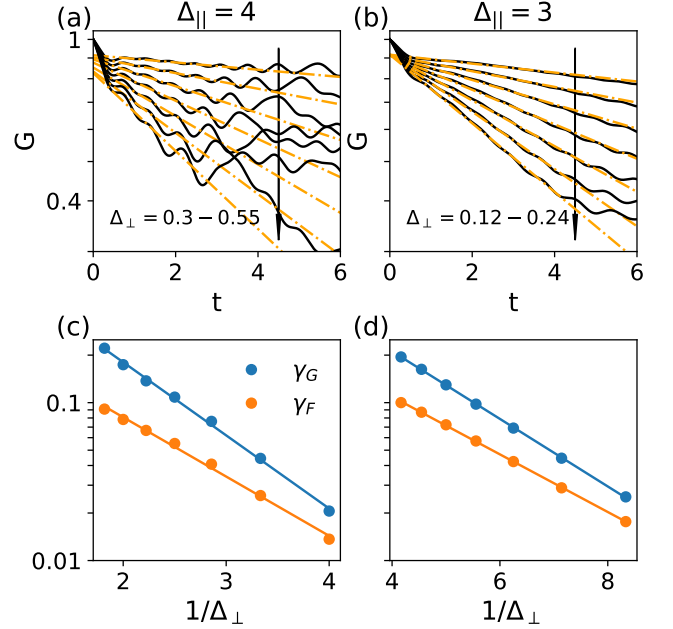


FIG. 4: *False vacuum decay for the XXZ ladder.* Panels (a) and (b): Time evolution of G in Eq. (5) after a quench $\Delta_{\perp} \rightarrow -\Delta_{\perp}$ with $\Delta_{||} = 4$ (a) and $\Delta_{||} = 3$ (b) with different values of Δ_{\perp} . In (a) $\Delta_{\perp} = 0.25, 0.3, 0.35, 0.4, 0.45, 0.5, 0.55$ while $\Delta_{\perp} = 0.12, 0.14, 0.16, 0.18, 0.20, 0.22, 0.24$ in (b). The arrows indicate the growing direction of Δ_{\perp} . Panels (c) and (d): decay rates extracted from the fits in (a) and (b), respectively, on semi-logarithmic scale. The continuous lines are fits of the decay rates performed according to Eq. (7)

ladder, we expect that the underlying mechanism of the false vacuum decay is the same so we can fit the decay rate with Eq. (7) with the replacement $h_z \rightarrow \Delta_\perp$. The test of this scaling for γ_G is presented in Fig. 4 c) and d), showing a perfect agreement. The quality of the fit for γ_F is very similar, although in Fig. 4 we only report the final values for γ_F and not the data for $F(t)$.

Conclusions and outlook— In this Letter we provided robust numerical evidence that for two one-dimensional spin models featuring confinement of elementary excitations it is possible to identify a range of physical parameters such that the rate of false vacuum decay is accessible in measurable time scales. The quench protocol that we described here is amenable to quantum simulation, for example with trapped ions or Rydberg atoms (both can simulate a system with confinement). For the false vacuum preparation, the imaginary time evolution used in the numerics can be replaced by an adiabatic preparation.

We conclude by briefly discussing how the trapped-ion quench experiment of Ref. [33] (for the observation of domain wall confinement in real time) can be adjusted to measure the false vacuum decay. In this experiment, the ion dynamics is well captured by a long-range quantum Ising model in which the \mathbb{Z}_2 symmetry is spontaneously (and not explicitly) broken. Hence, there are two degenerate real vacua and no false one. In order to get a phenomenology similar to our setup it is sufficient to slightly tilt the effective magnetic field (that in Ref. [33] is in the z direction) via a Rabi rotation, see the review [71]. This tilting provides a small component of the magnetic field along the x axis that breaks the degeneracy of the two vacua with a real and a false one. Then the preparation of the system in the false vacuum and the following quench are done with the very same techniques exploited already in Ref. [33]. Finally one- and two-point functions of the spin can be measured, as already done in Ref. [33], giving access to $F(t)$ and $G(t)$ in Eqs. (4) and (5).

Acknowledgments. We thank Guido Pagano, Marcello Dalmonte, and Gábor Takács for useful discussions. GL thanks BME and MK thanks SISSA for hospitality. We thank ERC for partial support under grant number 758329, AGEnTh, (FS) and 771536, NEMO, (GL and PC). MK acknowledges the Hungarian Quantum Technology National Excellence Program, project no. 2017-1.2.1- NKP- 2017-00001, and by the Fund TKP2020 IES (Grant No. BME-IE-NAT). MK acknowledges support by a Bolyai János grant of the HAS and by the ÚNKP-20-5 new National Excellence Program of the Ministry for Innovation and Technology from the source of the National Research, Development and Innovation Fund.

-
- [1] S. Coleman, *Fate of the false vacuum: Semiclassical theory*, *Phys. Rev. D* **15**, 2929 (1977), Erratum *Phys. Rev. D* **16**, 1248 (1977).
 - [2] C. G. Callan and S. Coleman, *Fate of the false vacuum. II. First quantum corrections*, *Phys. Rev. D* **16**, 1762 (1977).
 - [3] S. Coleman and F. De Luccia, *Gravitational effects on and of vacuum decay*, *Phys. Rev. D* **21**, 3305 (1980).
 - [4] M. S. Turner and F. Wilczek, *Is our vacuum metastable?*, *Nature* **298**, 633 (1982).
 - [5] U.-J. Wiese, *Ultracold quantum gases and lattice systems: quantum simulation of lattice gauge theories*, *Annalen der Physik* **525**, 777-796 (2013).
 - [6] M. Dalmonte and S. Montangero, *Lattice gauge theory simulations in the quantum information era* *Contemp. Phys.* **57**, 388-412 (2016).
 - [7] J. Preskill, *Simulating quantum field theory with a quantum computer*, *PoS LATTICE2018*, 024 (2019).
 - [8] M. C. Bañuls, R. Blatt, J. Catani, A. Celi, J. I. Cirac, M. Dalmonte, L. Fallani, K. Jansen, M. Lewenstein, S. Montangero, C. A. Muschik, B. Reznik, E. Rico, L. Tagliacozzo, K. Van Acoleyen, F. Verstraete, U.-J. Wiese, M. Wingate, J. Zakrzewski, and P. Zoller, *Simulating lattice gauge theories within quantum technologies*, *Eur. Phys. J. D* **74**, 165 (2020).
 - [9] T. M. R. Byrnes, P. Sriganesh, R. J. Bursill, and C. J. Hamer, *Density matrix renormalization group approach to the massive Schwinger model*, *Phys. Rev. D* **66**, 013002 (2002).
 - [10] M. C. Bañuls, K. Cichy, J. I. Cirac, K. Jansen, and H. Saito, *Matrix product states for lattice field theories*, *PoS LATTICE 2013*, 332 (2013).
 - [11] M. C. Bañuls, K. Cichy, J. I. Cirac, and K. Jansen, *The mass spectrum of the Schwinger model with matrix product states*, *J. High Energy Phys.* **11** (2013) 158.
 - [12] P. Silvi, E. Rico, T. Calarco, and S. Montangero, *Lattice gauge tensor networks*, *New J. Phys.* **16**, 103015, (2014).
 - [13] L. Tagliacozzo, A. Celi, and M. Lewenstein, *Tensor Networks for Lattice Gauge Theories with Continuous Groups*, *Phys. Rev. X* **4**, 041024 (2014).
 - [14] B. Buyens, J. Haegeman, K. Van Acoleyen, H. Verschelde, and F. Verstraete *Matrix Product States for Gauge Field Theories*, *Phys. Rev. Lett.* **113**, 091601 (2014).
 - [15] E. Rico, T. Pichler, M. Dalmonte, P. Zoller, and S. Montangero, *Tensor Networks for Lattice Gauge Theories and Atomic Quantum Simulation*, *Phys. Rev. Lett.* **112**, 201601 (2014).
 - [16] M. C. Bañuls and K. Cichy, *Review on novel methods for lattice gauge theories*, *Rep. Prog. Phys.* **83** 024401 (2020).
 - [17] E. Zohar, J. I. Cirac, and B. Reznik, *Simulating Compact Quantum Electrodynamics with Ultracold Atoms: Probing Confinement and Nonperturbative Effects*, *Phys. Rev. Lett.* **109**, 125302 (2012).
 - [18] D. Banerjee, M. Bögli, M. Dalmonte, E. Rico, P. Stebler, U.-J. Wiese, and P. Zoller *Atomic Quantum Simulation of $U(N)$ and $SU(N)$ Non-Abelian Lattice Gauge Theories*, *Phys. Rev. Lett.* **110**, 125303 (2013).
 - [19] A. Mezzacapo, E. Rico, C. Sabín, I. L. Egusquiza, L. Lamata, and E. Solano, *Non-Abelian $SU(2)$ Lattice Gauge Theories in Superconducting Circuits*, *Phys. Rev.*

- Lett. **115**, 240502 (2015).
- [20] E. A. Martinez, C. A. Muschik, P. Schindler, D. Nigg, A. Erhard, M. Heyl, P. Hauke, M. Dalmonte, T. Monz, P. Zoller, and R. Blatt, *Real-time dynamics of lattice gauge theories with a few-qubit quantum computer*, *Nature* **534**, 516 (2016).
 - [21] F. M. Surace, P. P. Mazza, G. Giudici, A. Lerose, A. Gambassi, and M. Dalmonte, *Lattice Gauge Theories and String Dynamics in Rydberg Atom Quantum Simulators*, *Phys. Rev. X* **10**, 021041 (2020).
 - [22] Y. Atas, J. Zhang, R. Lewis, A. Jahanpour, J. F. Haase, and C. A. Muschik, *SU(2) hadrons on a quantum computer*, [arxiv:2102.08920](#).
 - [23] Z. Davoudi, N. M. Linke, and G. Pagano, *Toward simulating quantum field theories with controlled phonon-ion dynamics: A hybrid analog-digital approach*, [arxiv:2104.09346](#).
 - [24] T. P. Billam, R. Gregory, F. Michel, and I. G. Moss, *Simulating seeded vacuum decay in a cold atom system*, *Phys. Rev. D* **100**, 065016 (2019).
 - [25] T. P. Billam, K. Brown, and I. G. Moss, *Simulating cosmological supercooling with a cold-atom system*, *Phys. Rev. A* **102**, 043324 (2020).
 - [26] S. Abel and M. Spannowsky, *Quantum-Field-Theoretic Simulation Platform for Observing the Fate of the False Vacuum*, *PRX Quantum* **2**, 010349 (2021).
 - [27] K. L. Ng, B. Opanchuk, M. Thenabadu, M. Reid, and P. D. Drummond, *Fate of the False Vacuum: Finite Temperature, Entropy, and Topological Phase in Quantum Simulations of the Early Universe*, *PRX Quantum* **2**, 010350 (2021).
 - [28] T. P. Billam, K. Brown, A. J. Groszek, and I. G. Moss, *Simulating cosmological supercooling with a cold atom system II*, [arxiv:2104.07428](#).
 - [29] B. M. McCoy and T. T. Wu, *Two-dimensional Ising field theory in a magnetic field: Breakup of the cut in the two-point function*, *Phys. Rev. D* **18**, 1259 (1978).
 - [30] N. Ishimura and H. Shiba, *Dynamical Correlation Functions of One-Dimensional Anisotropic Heisenberg Model with Spin 1/2. I: Ising-Like Antiferromagnets*, *Progr. Theor. Phys.* **63**, 743 (1980); H. Shiba, *Quantization of Magnetic Excitation Continuum due to Interchain Coupling in Nearly One-Dimensional Ising-like Antiferromagnets*, *Theor. Phys.* **64**, 743 (1980).
 - [31] M. Kormos, M. Collura, G. Takács, and P. Calabrese, *Real-time confinement following a quantum quench to a non-integrable model*, *Nat. Phys.* **13**, 246 (2016).
 - [32] F. Liu, R. Lundgren, P. Titum, G. Pagano, J. Zhang, C. Monroe, and A. V. Gorshkov, *Confined Quasiparticle Dynamics in Long-Range Interacting Quantum Spin Chains*, *Phys. Rev. Lett.* **122**, 150601 (2019).
 - [33] W. L. Tan, P. Becker, F. Liu, G. Pagano, K. S. Collins, A. De, L. Feng, H. B. Kaplan, A. Kyprianidis, R. Lundgren, W. Morong, S. Whitsitt, A. V. Gorshkov, and C. Monroe, *Observation of Domain Wall Confinement and Dynamics in a Quantum Simulator*, *Nature Phys.* **17**, 742 (2021).
 - [34] F. M. Surace and A. Lerose, *Scattering of mesons in quantum simulators*, *New J. Phys.* **23** (2021) 062001.
 - [35] R. J. Valencia Tortora, P. Calabrese, and M. Collura, *Relaxation of the order-parameter statistics and dynamical confinement*, *EPL* **132**, 50001 (2020).
 - [36] P. I. Karpov, G.-Y. Zhu, M. P. Heller, and M. Heyl, *Spaciotemporal dynamics of particle collisions in quantum spin chains*, [arxiv:2011.11624](#).
 - [37] A. Milsted, J. Liu, J. Preskill, and G. Vidal, *Collisions of false-vacuum bubble walls in a quantum spin chain*, [arxiv:2012.07243](#).
 - [38] A. Sinha, T. Chanda, and J. Dziarmaga, *Nonadiabatic dynamics across a first-order quantum phase transition: Quantized bubble nucleation*, *Phys. Rev. B* **103**, L220302 (2021).
 - [39] M. Rigobello, S. Notarnicola, G. Magnifico, and S. Montangero, *Entanglement generation in QED scattering processes*, [arxiv:2105.03445](#).
 - [40] S. Sachdev, *Quantum Phase Transitions*, Cambridge University Press (2001).
 - [41] G. Mussardo, *Statistical field theory: an introduction to exactly solved models in statistical physics*, 2nd edition, Oxford University Press (2020).
 - [42] Z. Cai, C. Wu, and U. Schollwöck, *Confinement: A real-time visualization*, *Phys. Rev. B* **85**, 075102 (2012).
 - [43] T. Rakovszky, M. Mestyan, M. Collura, M. Kormos, and G. Takács, *Hamiltonian truncation approach to quenches in the Ising field theory*, *Nucl. Phys. B* **911**, 805 (2016).
 - [44] A. J. A. James, R. M. Konik, and N. J. Robinson, *Non-thermal States Arising from Confinement in One and Two Dimensions*, *Phys. Rev. Lett.* **122**, 130603 (2019).
 - [45] N. J. Robinson, A. J. A. James, and R. M. Konik, *Signatures of rare states and thermalization in a theory with confinement*, *Phys. Rev. B* **99**, 195108 (2019).
 - [46] P. P. Mazza, G. Peretto, A. Lerose, M. Collura, and A. Gambassi, *Suppression of transport in nondisordered quantum spin chains due to confined excitations*, *Phys. Rev. B* **99**, 180302(R) (2019).
 - [47] O. A. Castro-Alvaredo, M. Lencsés, I. M. Szécsényi, and J. Viti, *Entanglement oscillations near a quantum critical point*, *Phys. Rev. Lett.* **124**, 230601 (2020).
 - [48] J. Vovrosh and J. Knolle, *Confinement Dynamics on a Digital Quantum Computer*, *Sci. Rep.* **11**, 11577 (2021).
 - [49] R. C. Myers, M. Rozali, and B. Way, *Holographic quenches in a confined phase*, *J. Phys. A* **50**, 494002 (2017).
 - [50] A. Cortes Cubero and N. J. Robinson, *Lack of thermalization in (1+1)-d quantum chromodynamics at large N_c* , *J. Stat. Mech.* (2019) 123101.
 - [51] Z.-C. Yang, F. Liu, A. V. Gorshkov, and T. Iadecola, *Hilbert-Space Fragmentation from Strict Confinement*, *Phys. Rev. Lett.* **124**, 207602 (2020).
 - [52] S. Pai and M. Pretko, *Fractons from confinement in one dimension*, *Phys. Rev. Res.* **2**, 013094 (2020).
 - [53] S. B. Rutkevich, *Decay of the metastable phase in $d = 1$ and $d = 2$ Ising models*, *Phys. Rev. B* **60**, 14525 (1999).
 - [54] D. Banerjee, M. Dalmonte, M. Müller, E. Rico, P. Stebler, U.-J. Wiese, and P. Zoller, *Atomic Quantum Simulation of Dynamical Gauge Fields Coupled to Fermionic Matter: From String Breaking to Evolution After a Quench*, *Phys. Rev. Lett.* **109**, 175302 (2012).
 - [55] F. Hebenstreit, J. Berges, and D. Gelfand, *Real-Time Dynamics of String Breaking*, *Phys. Rev. Lett.* **111**, 201601 (2013).
 - [56] S. Kühn, E. Zohar, J. I. Cirac, and M. C. Banuls, *Non-abelian string breaking phenomena with matrix product states*, *J. High Energy Phys.* **07** (2015) 130.
 - [57] T. Pichler, M. Dalmonte, E. Rico, P. Zoller, and S. Montangero, *Real-Time Dynamics in $u(1)$ Lattice Gauge Theories with Tensor Networks*, *Phys. Rev. X* **6**, 011023 (2016).
 - [58] V. Kasper, F. Hebenstreit, M. K. Oberthaler, and J.

- Berges, *Schwinger pair production with ultracold atoms*, *Phys. Lett. B* **760**, 742 (2016).
- [59] B. Buyens, J. Haegeman, F. Hebenstreit, F. Verstraete, and K. Van Acoleyen, *Real-time simulation of the Schwinger effect with matrix product states*, *Phys. Rev. D* **96**, 114501 (2017).
- [60] Y. Kuno, S. Sakane, K. Kasamatsu, I. Ichinose, and T. Matsui, *Quantum simulation of $(1+1)$ -dimensional $U(1)$ gauge-Higgs model on a lattice by cold bose gases*, *Phys. Rev. D* **95**, 094507 (2017).
- [61] P. Sala, T. Shi, S. Kühn, M. C. Bañuls, E. Demler, and J. I. Cirac, *Variational study of $U(1)$ and $SU(2)$ lattice gauge theories with gaussian states in $1+1$ dimensions*, *Phys. Rev. D* **98**, 034505 (2018).
- [62] D. Spitz and J. Berges, *Schwinger pair production and string breaking in non-abelian gauge theory from real-time lattice improved hamiltonians*, *Phys. Rev. D* **99**, 036020 (2019).
- [63] J. Park, Y. Kuno, and I. Ichinose, *Glassy dynamics from quark confinement: Atomic quantum simulation of the gauge-Higgs model on a lattice*, *Phys. Rev. A* **100**, 013629 (2019).
- [64] G. Magnifico, M. Dalmonte, P. Facchi, S. Pascazio, F. V. Pepe, and E. Ercolessi, *Real time dynamics and confinement in the \mathbb{Z}_n Schwinger-Weyl lattice model for $1+1$ QED*, *Quantum* **4**, 281 (2020).
- [65] S. Notarnicola, M. Collura, and S. Montangero, *Real time dynamics quantum simulation of $(1+1)$ -d lattice QED with Rydberg atoms*, *Phys. Rev. Res.* **2**, 013288 (2020).
- [66] T. Chanda, J. Zakrzewski, M. Lewenstein, and L. Tagliacozzo, *Confinement and Lack of Thermalization After Quenches in the Bosonic Schwinger Model*, *Phys. Rev. Lett.* **124**, 180602 (2020).
- [67] A. Lerose, F. M. Surace, P. P. Mazza, G. Peretto, M. Collura, and A. Gambassi, *Quasilocalized dynamics from confinement of quantum excitations*, *Phys. Rev. B* **102**, 041118(R) (2020).
- [68] R. Verdel, F. Liu, S. Whitsitt, A. V. Gorshkov, and M. Heyl, *Real-time dynamics of string breaking in quantum spin chains*, *Phys. Rev. B* **102**, 014308 (2020).
- [69] O. Pomponio, M.A. Werner, G. Zarand, and G. Takács, *Bloch oscillations and the lack of the decay of the false vacuum in a one-dimensional quantum spin chain*, *arxiv:2105.00014*.
- [70] G. Lagnese, F. M. Surace, M. Kormos, and P. Calabrese, *Confinement in the spectrum of a Heisenberg-Ising spin ladder*, *J. Stat. Mech.* (2020) 093106.
- [71] C. Monroe, W. C. Campbell, L.-M. Duan, Z.-X. Gong, A. V. Gorshkov, P. W. Hess, R. Islam, K. Kim, N. M. Linke, G. Pagano, P. Richerme, C. Senko, and N. Y. Yao, *Programmable quantum simulations of spin systems with trapped ions*, *Rev. Mod. Phys.* **93**, 025001 (2021).
- [72] In Ref. 53, the rate γ contains an oscillatory term $g(h_z)$: we work here in the approximation $g(h_z) \simeq 1$, which is justified for h_z sufficiently far from 1.